

One-Inductor Single-stage Differential Boost Inverter Operated in Discontinuous Current Mode for Single-Phase Grid-Tied Photovoltaic System

Ayato Sagehashi, Le Hoai Nam and Jun-ichi Itoh

Department of Electrical Engineering
Nagaoka University of Technology, NUT
Nagaoka, Niigata, Japan

sagehashi@stn.nagaokaut.ac.jp, lehoainam@stn.nagaokaut.ac.jp, itoh@vos.nagaokaut.ac.jp

Abstract—In this paper, a novel single-stage boost inverter using one inductor is proposed for a grid-tied photovoltaic (PV) inverter. The proposed inverter shares one inductor with two boost converters by utilizing discontinuous current mode (DCM). The output voltage is controlled by the differential voltage between boost converters. Using this topology, the neutral point of the grid can be connected to a terminal of the solar panel. As a result, common-mode noise can be suppressed. The operation of the proposed inverter is confirmed with 100-W prototype with a DC input voltage of 100 V and an AC output voltage of 100 V. The output current THD is 1.4%.

Keywords—DC/AC converter, Discontinuous current mode, Micro-inverter

I. INTRODUCTION

In recent years, PV systems have been widely used as an alternative power supply from natural energy. In such system, the PV inverter is required for interconnecting the grid and the PV system. In particular, the PV inverter is strongly required to minimize and achieve high efficiency[1]-[5]. The generated power of the PV system depends heavily on the weather condition and the solar radiation. Therefore, in the conventional PV systems where only one inverter is connected with several solar panels, if only one solar panel is shaded by clouds or rain, the output power of the whole system worsens. In order to solve this problem, a micro-inverter has been proposed as an alternative method for PV inverter [6]-[10]. In particular, each micro-inverters are connected to each solar panels separately. Therefore, the generated power will be increased in partial shadow condition because the generated power of each solar panel is controlled independently. Consequently, problems on individual solar panels does not influence heavily on the operation of the whole system. However, the minimization of the micro-inverter is necessary in terms of the installation area in order to connect to each solar panel separately.

One of the main factors preventing the minimization of the micro-inverter is the passive components, i.e. the inductor and the capacitor. In general, the PV inverter is composed of a boost converter and an inverter. The boost converter is used to

control the DC-link voltage, whereas the inverter converts the DC power to AC power. In this case, a high-voltage DC-link capacitor is required with a large capacitance, which absorbs a power fluctuation caused by the single-phase grid. On the other hand, the system volume of the DC/AC converter increases because an boost inductor of a boost converter and interconnected inductors of an inverter are necessary.

On the other hand, the single-stage boost inverter for the DC/AC converters have been proposed in order to unify the boost converter and the inverter [11]-[15]. The single-stage boost inverter can reduce the number of the switching devices and the inductors. It is two inductors for the boost operation and four switching devices compose two boost converter circuits. Therefore, the single-stage boost inverter can be minimized due to the reduction of circuit elements compared with the typical DC/AC topology. In addition, the leak current caused by the floating capacitance between the solar panel and the ground is significantly reduced due to the voltage fluctuation at the neutral point is small between the solar panel and the grid. However, the single-stage boost inverter still use two inductors. Consequently, the number of the inductor is necessary to further reduce in order to minimize the circuit volume.

In this paper, a novel boost inverter is proposed in order to convert from DC to AC including the boost operation using only one small input inductor. First, the conventional two stage DC/AC converter for the PV system, the conventional single-stage boost inverter and the proposed boost inverter are explained. Secondly, the operation modes and switching patterns of the proposed boost inverter is shown. Third, the input inductor current control and the output capacitor voltage control are explained. In addition, the calculation method of each duty ratio command values for DCM is established. Fourth, the operation of the proposed boost inverter by simulation after the design method of the input inductor at the critical mode of DCM is confirmed. Next, the losses of the switching devices and inductors are compared between the conventional two stage DC/AC converter and the proposed boost inverter. Finally, the operation of the proposed inverter is confirmed in experiment. As a result, the conversion from DC

to AC is realized by the proposed boost inverter which reduces the number of inductors compared with the conventional two-stage DC/AC converter and the conventional single-stage boost inverter.

II. DC/AC CONVERTER TOPOLOGY

A. Conventional two-stage AC/DC converter

Fig. 1 shows the conventional two stage DC/AC converter topology for the PV inverter. The conventional two stage DC/AC converter is composed the boost converter and the H-bridge inverter in order to convert from DC to AC. The DC link voltage requires the higher voltage than the maximum grid voltage when the inverter is connected to the grid. Therefore, the large capacitor is necessary to connect between the boost converter and the inverter when the input voltage is lower than the grid voltage. Additionally, the boost inductor and the interconnected inductors prevent in order to minimize the system. As a result, a number of passive components, switching devices and the value of the capacitance are required to reduce in order to minimize the system of the conventional two stage DC/AC converter.

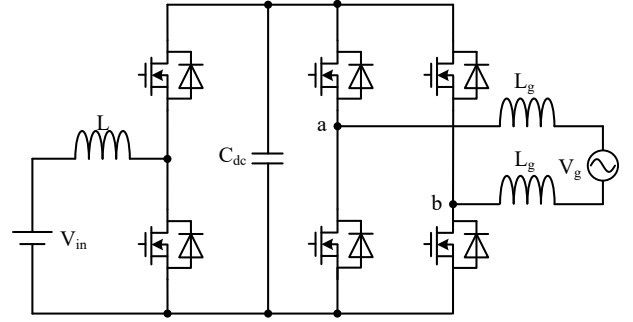


Fig. 1. Conventional two-stage DC/AC converter.

B. Conventional single-stage boost inverter

Fig. 2 shows the conventional single-stage differential boost inverter. Two boost converters compose the conventional single-stage differential boost inverter. This inverter regulates the voltage of output side capacitors V_{Ca} and V_{Cb} to sinusoidal waveform including the offset voltage higher than the input voltage. In addition, the output current is controlled by potential differences of the output capacitors. Therefore, compared to the conventional two stage DC/AC converter, the conventional single-stage boost inverter requires only four switches and two inductors. In this case, the total volume of the boost inductors of the single-stage boost inverter is smaller than that of the conventional two stage DC/AC converter. However, it is necessary to further reduce the number of the inductors in order to minimize the system volume.

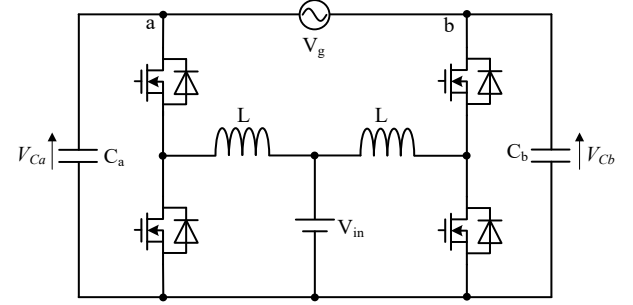


Fig. 2. Conventional single-stage differential boost inverter.

C. Proposed single-phase boost inverter

Fig. 3 shows the circuit diagram of the proposed single-phase boost inverter. In principle, the proposed boost inverter is combined of two boost converter, requiring a switching device and two bidirectional switches. Note that if only typical unidirectional switches are used, the proposed boost inverter requires more switching devices compared with the conventional single-stage boost inverter. On the other hand, the proposed boost inverter is operated in DCM. Consequently, the number of the input inductor is reduced to only one because the input inductor current is shared for the voltage control of each output capacitor C_a and C_b . Hence, the converter size can be reduced. Furthermore, the number of the switching devices of the proposed inverter can be reduced to only three if the bidirectional switches can be employed with GaN-based monolithic bidirectional switches, which has same on resistance as the unidirectional switches [16].

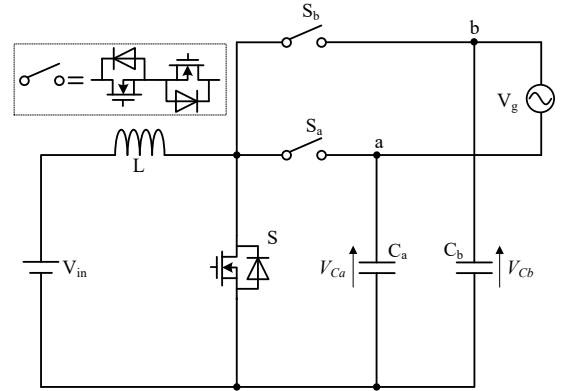


Fig. 3. Proposed single-stage differential boost inverter.

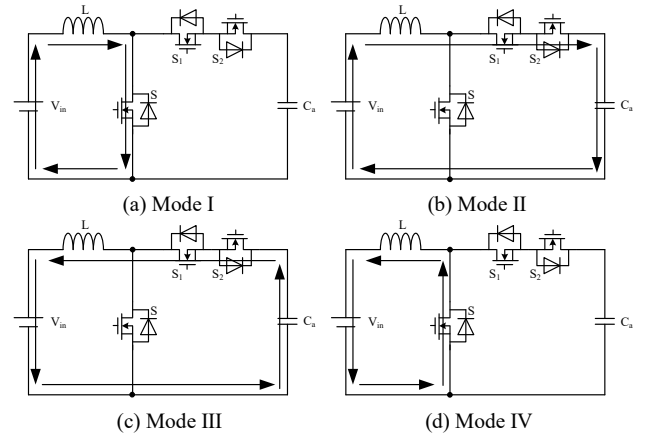


Fig. 4. Operation mode for each capacitor voltage control.

Fig. 4 shows the operation mode of the proposed boost inverter. The operation mode is shown only the output

capacitor C_a caused by the operation mode of the output capacitor C_b similarly. The output capacitor voltages are controlled similar to the boost operation and the step-down operation. The input inductor current is controlled to positive direction at Mode I and II periods. At Mode III and IV, the input inductor current is controlled to negative direction in order to get the desired output capacitor voltage V_{Ca} . In this operation mode, the boost inverter operate the boost mode when the output current command value is positive. The operation is the step-down mode when the other direction of the output current command value. Furthermore, the sinusoidal waveform of the output side is realized by the differential voltage between output capacitor voltages V_{Ca} and V_{Cb} which is controlled to inverse phase.

III. CONTROL METHOD FOR BOOST INVERTER

Fig. 5 shows the voltage control block for the output capacitor C_a in the boost inverter. The PI controller controls only the average voltage of the output capacitor C_a . In addition, the output current command is added to the inductor current command value in the minor loop as a feed forward regulation in order to control the output current [17]. The output capacitor voltage is necessary to be higher than the input voltage in order to achieve the sinusoidal waveform at the output side of boost inverter. Hence, the output capacitor voltage command value must satisfy (1).

$$V_{C_{a_avg}} > \frac{V_{out_peak}}{2} + V_{in} \quad (1)$$

where $V_{C_{a_avg}}$ is the output capacitor voltage command value, V_{out_peak} is the maximum amplitude of the grid voltage, V_{in} is the input voltage. The input inductor current command value is calculated after deciding the output capacitor voltage command value by (1). The input inductor current command value is decided by (2)

$$i_{La}^* = (i_{Ca} + i_{out}^*) \frac{V_{Ca}}{V_{in}} = \left[i_{Ca} + \frac{P_{out}}{V_{out_rms}} \sqrt{2} \sin(2\pi f_{out} t) \right] \frac{V_{Ca}}{V_{in}} \quad (2)$$

where i_{Ca} is the output capacitor command value voltage control, i_{out}^* is the output current command value, V_{Ca} is the output capacitor voltage, P_{out} is the output power, V_{out_rms} is the effective value of the grid voltage, f_{out} is the frequency of the grid. Note that the input inductor current command value for the other output capacitor voltage V_{Cb} is omitted due to explanation by inverting the output current command value. The duty of the boost inverter is then compared with sawtooth waveform to generate the switching signal.

Fig. 6 shows the relationship between the input inductor current and the duty ratio of the boost inverter. Duty ratio command values d_1 and d_2 are the period for the control of the output capacitor voltage V_{Ca} . Duty ratio command values d_3 and d_4 are the period for the control of the output capacitor voltage V_{Cb} . These duty ratio command values are controlled in order to share the input inductor current. Furthermore, the duty ratio command value d_0 is the zero current period in order to

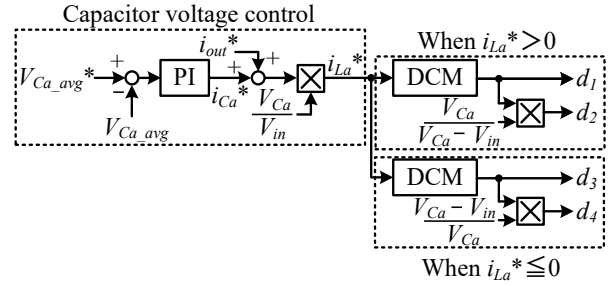


Fig. 5. Control block for output capacitor C_a voltage control.

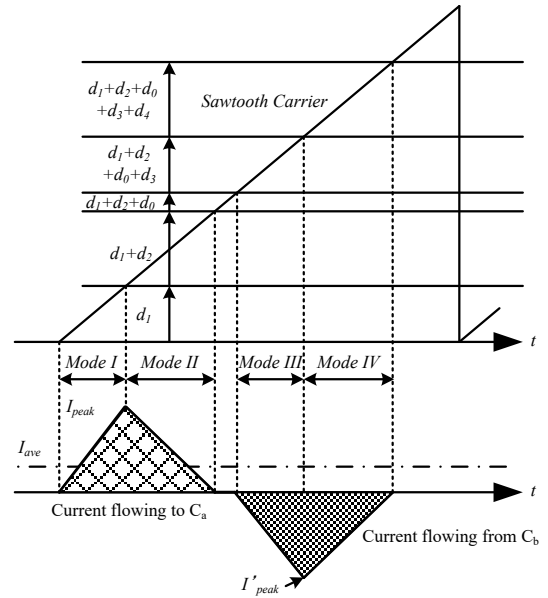


Fig. 6. Waveform of relationship between inductor current and duty ratio.

prevent the interference of the current control between the output capacitor C_a and C_b .

The duty ratio for the input inductor current control is calculated by the relationship between the maximum value and the average value of the input inductor current. In the control of the output capacitor voltage V_{Ca} , the maximum value and the average value of the input inductor current is shown by (3) and (4).

$$I_{peak_Vca} = \frac{V_{in}}{L} d_1 T_{sw} = \frac{V_{Ca} - V_{in}}{L} d_2 T_{sw} \quad (3)$$

$$I_{ave_Vca} = \frac{I_{peak_Vca}}{2} (d_1 + d_2) \quad (4)$$

where L is the input inductor, d_1 and d_2 are the duty ratio in Fig. 6. The relationship between d_1 and d_2 is calculated by the maximum value and the average value of the input inductor current. The duty ratios d_1 and d_2 are explained by (5) and (6).

$$d_1 = \sqrt{\frac{2L(V_{Ca} - V_{in})}{V_{in}V_{Ca}T_{sw}}} i_{ave_Ca} = \sqrt{\frac{2\sqrt{2}P_{out}L(V_{Ca} - V_{in})}{V_{in}^2V_{out_rms}T_{sw}}} \quad (5)$$

$$d_2 = \frac{V_{in}}{V_{Ca} - V_{in}} d_1 \quad (6)$$

The inductor current is controlled to the DCM by duty ratio. Similarly, in based on the output capacitor voltage V_{Cb} , the duty ratio of the input inductor current d_3 and d_4 is calculated by (7) and (8).

$$d_3 = \sqrt{\frac{2LV_{in}}{(V_{Cb} - V_{in})V_{Cb}T_{sw}}} i_{ave_Cb} = \sqrt{\frac{2\sqrt{2}P_{out}L}{(V_{Cb} - V_{in})V_{out_rms}T_{sw}}} \quad (7)$$

$$d_4 = \frac{V_{Cb} - V_{in}}{V_{in}} d_3 \quad (8)$$

As a result, the DCM operation of the input inductor current is achieved. In addition, the input inductor current share each operation mode in input inductor.

IV. CONSIDERATION OF INDUCTOR

A. Design of input inductor for boost inverter

Fig. 7 shows the waveform of the input voltage V_{in} , output capacitor voltages V_{Ca} and V_{Cb} in the boost inverter. In this case, the average output capacitor voltages are decided by (1). Furthermore, each output capacitor voltages have a margin V_{out_margin} in order to prevent the input voltage and output capacitor voltages from becoming same voltage.

The boost inverter shares the current of each operation modes on only one input inductor. Therefore, the duty command values of operation modes are satisfied (9).

$$d_1 + d_2 + d_3 + d_4 = 1 \quad (9)$$

In this case, the condition is the critical mode; i.e. it is the worst case at the DCM operation of the inductor current. Note that the duty command value of the zero current period d_0 is added to (9) if the zero current is necessary. The conduction loss of switching devices can be reduced due to the current ripple of the inductor current is the minimum at the critical mode of the DCM operation. Hence, the best condition for the input inductor is the critical mode of DCM operation at the rated power. The input inductor value of the critical mode is designed by (10) which are relationship between duty command values from (5) to (8) and the condition of the critical mode (9).

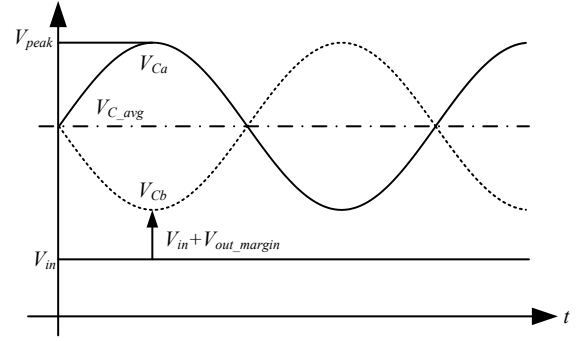


Fig. 7. Relationship between input voltage and output capacitor voltage at inductor design.

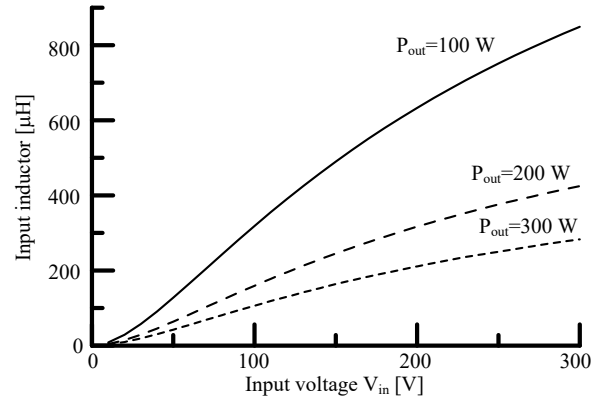


Fig. 8. Designed inductor value of boost inverter at critical mode of DCM (include 10% margin).

$$L = \frac{V_{in}^2 V_{out_rms} T_{sw}}{2\sqrt{2}P_{out} \left(\frac{V_{Ca}}{\sqrt{V_{Ca} - V_{in}}} + \frac{V_{Cb}}{\sqrt{V_{Cb} - V_{in}}} \right)^2} \quad (10)$$

where V_{g_rms} is the effective value of the grid voltage, P_{out} is the output power, T_{sw} is the switching period of the boost inverter. Moreover, the input inductor value have a 10% margin compared with the design value when the prototype circuit of the boost inverter use the input inductor designing by (10).

Fig.8 show the designing inductor value when the input voltage is changed at each output power conditions. The design conditions are 200 V of the grid voltage and 10 kHz of the switching frequency. In addition, the minimum voltage of the output capacitor is higher than the input voltage by 20% of the maximum value of the grid voltage. The input inductor is increased when the input voltage is increased. On the other hand, the input inductor value become small when the output power become high.

B. Inductor comparison with conventional system

The value of the input inductor for boost inverter is under mH when the input voltage is changed. Therefore, it is considered how the input inductor of the boost inverter can be decreased compared with the conventional two-stage system.

Fig. 9 shows the structure of the inductor when inductors are designed. Table 1 shows the design condition of circuit parameters and material parameters about circuit specification and the inductor core. The Ferrite is selected for the material of the inductor core. In addition, the shape of the inductor core is EE type. The space factor is supposed from 0.4 to 0.6 at the design of the inductor. The boost inductor of the conventional two stage type is designed by the ripple current value of the inductor. Therefore, it is designed by (11).

$$L = \frac{V_{in}}{\Delta I_L f_{sw}} \frac{V_{DC} - V_{in}}{V_{DC}} \quad (11)$$

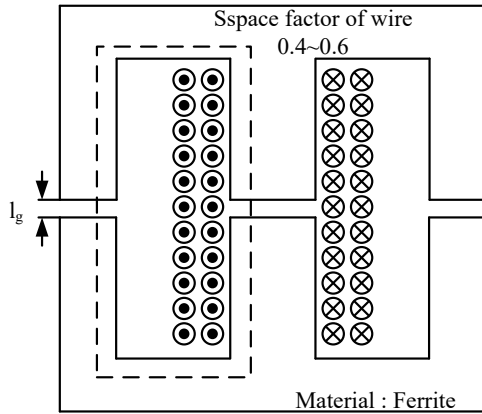


Fig. 9. Designing inductor structure of each circuit topology.

Table 1 Design condition of inductors

Material condition of Inductor	Shape type	EE core
	Material	N87
Design condition of conventional circuit	Initial permeability μ_i	2200 \pm 25%
	Flux density B_s	490 mT
	Flux density H_s	21 A/m
	Resistivity ρ	10 Ω m
	Output power P_{out}	300 W
Circuit condition	Output voltage V_{out}	200 V
	Switching frequency f_{sw}	10 kHz
Design condition of conventional circuit	DC link voltage V_{DC}	350 V
	Ripple ratio of current ΔI_L	30 %

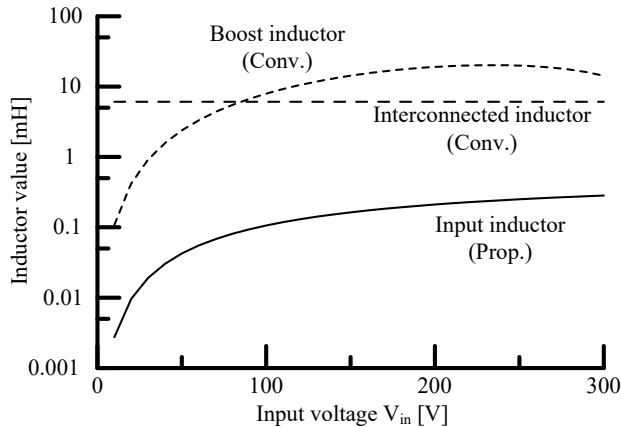


Fig. 10. Comparison of designed inductor values between conventional two-stage type and boost inverter when the input voltage is changed.

where V_{in} is the input voltage, V_{DC} is the DC link voltage, f_{sw} is the switching frequency, ΔI_L is the ripple current of the inductor at peak to peak. The interconnected inductor of the conventional two stage type is also designed by (11). V_{in} is the peak voltage of the grid when the interconnected inductor is designed. In addition, f_{sw} is two times compared with boost inductor design due to the inverter is operated at PWM.

Fig. 10 shows design inductor values of the conventional two stage type and the boost inverter. The boost inductor and the interconnected inductor are 2.21 mH and 6.1 mH at the input voltage is 48 V. On the other hand, the input inductor of the boost inverter is 40.1 μ H. The input inductor value of the boost inverter is reduced by 98.2% compared with the boost inductor of the conventional two stage type. In addition, the effect for minimization is large due to the conventional two stage type have the interconnected inductor without the boost inductor. As a result, the boost inverter can reduce the circuit volume compared with the conventional two stage type.

V. SIMULATION RESULTS

A. Operation of boost inverter

Table 2 shows the simulation conditions, whereas Fig. 11

Table 2. Simulation conditions of boost inverter.

Specification	Output power P_{out}	300 W
	Output voltage V_{out}	200 V
	Output frequency f_{out}	50 Hz
	Input voltage V_{in}	48 V
Conventional circuit	Boost inductor	2.2 mH
	Interconnected inductor	6.1 mH
Boost inverter	Boost inductor	40 μ H

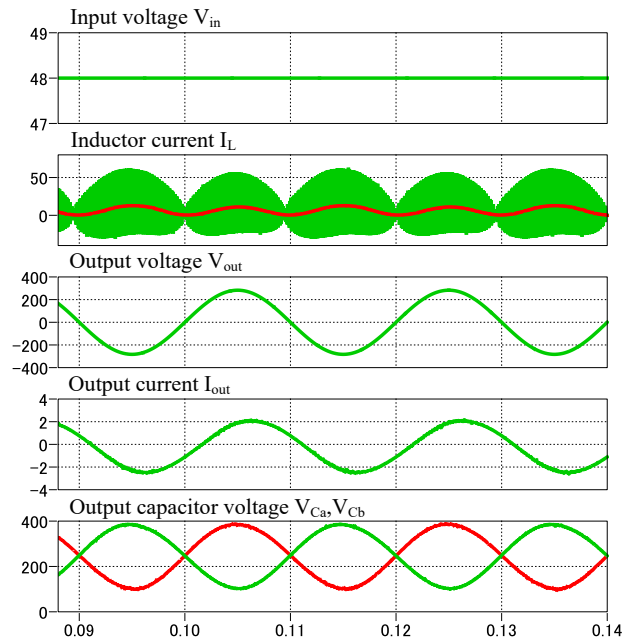


Fig. 11. Operation each waveform of boost inverter circuit in simulation.

shows the simulation results of the boost inverter operation. It is confirmed that the boost inverter can generate the sinusoidal waveform of the output voltage when the input power supply is DC source. In addition, the voltage of the output capacitor V_{Ca} and V_{Cb} is controlled over the input voltage at each operation mode periods. In consequence, the boost inverter is achieved the boost mode and the step-down mode.

Fig. 12 shows the magnified waveform of the input inductor current. It is confirmed the input inductor current is operated in each period for the voltage of the output capacitor V_{Ca} and V_{Cb} . As a result, the input current is realized DCM operation in order to share the input inductor current for each operation mode. In this simulation, the input inductor current have the zero current period between the voltage control of V_{Ca} and V_{Cb} .

Fig. 13 shows the neutral point voltage waveform of the grid side at the operating boost inverter in simulation. The neutral point voltage is kept the constant value by the average value of the output capacitor voltage. Additionally, the voltage ripple of the neutral point voltage is under the 10 V. As a result, the voltage changing of the grid side is suppressed due to the voltage ripple of the neutral point voltage is low.

B. Loss analysis

Fig. 14 shows simulation results of the loss analysis. It is compared with two DC/AC converters, the conventional two stage type and the boost inverter. In this case, the loss analysis results include only the switching devices and the inductor. The inductor loss is obtained from GeckoMAGNETICS of the simulation software. From the results, the loss of the boost inverter is reduced compared with the conventional two-stage

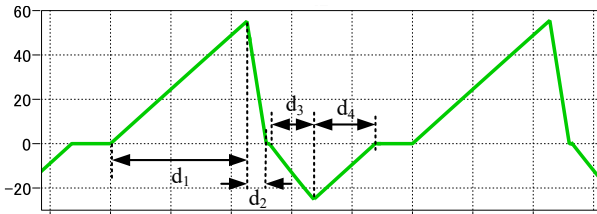


Fig. 12. Magnifying operation waveform of input inductor current.

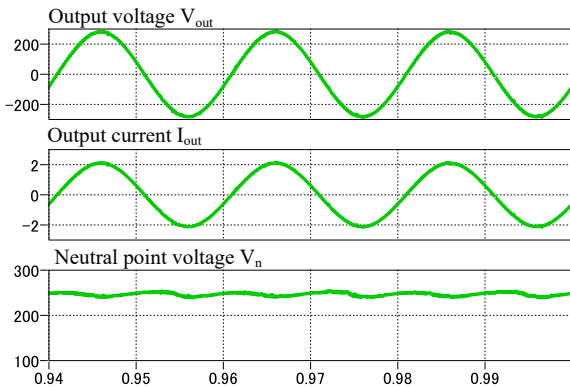


Fig. 13. Measurement waveform of neutral point voltage of proposed circuit.

type. The switching device losses of the conventional type are 4.7 W. The loss of the boost inverter is 7.6 W. The switching device losses of the boost inverter are 38.2% larger than conventional two stage type. It is caused by the large effective value of the input inductor current of the boost inverter compared with the conventional two stage type. On the other hand, inductor losses are 13.7 W of the conventional two stage type due to the inductor is connected to boost converter side and inverter side. In the boost inverter, the inductor loss is 6.6 W caused by connecting the small inductor. Therefore, the inductor loss of the boost inverter is 51.8% smaller than the conventional two stage type. As a results, the converter loss of the boost inverter can be reduced compared with the conventional two stage type due to the inductor current is shared in boost inverter.

Fig. 15 shows the RMS inductor current for each inductors. These are the boost inductor and the interconnected inductor of the conventional two stage type compared with the input inductor of the boost inverter. The boost inductor current is 6.5 A at 48 V of the input voltage. Additionally, the interconnected inductor current is 1.5 A. On the other hand, the input inductor

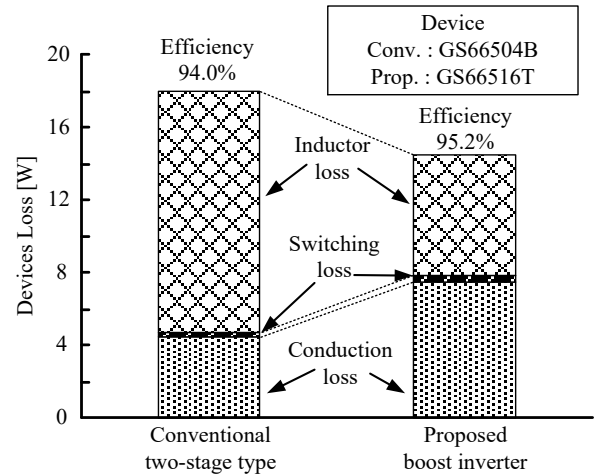


Fig. 14. Loss analysis of conventional circuit and proposed circuit in simulation.

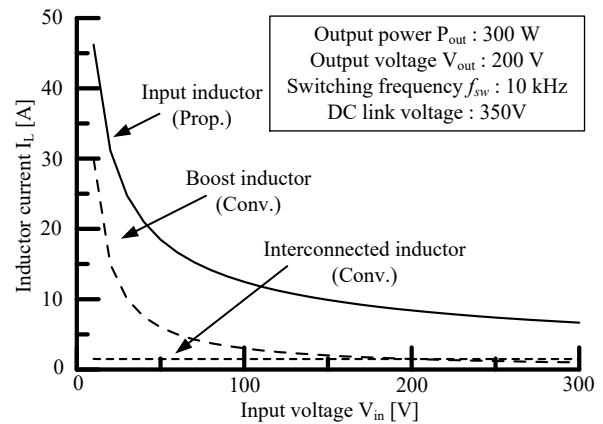


Fig. 15. Comparison of RMS of each inductor current.

current is 20 A. It is 67.5% large compared with the boost inductor current. Therefore, it is confirmed the effective current in the boost inverter is large compared with the conventional two stage type. In consequence, the loss of the switching device is increased in the boost inverter. However, the inductor loss of the boost inverter is reduced due to the inductor value of the boost inverter is smaller than each inductor of the conventional two stage type.

C. Inductor energy of boost inverter

Fig. 16 shows the inductor energy of each inductor of the conventional two stage type and the boost inverter. Energies of the boost inductor and the interconnected inductor are 43.2 mJ and 6.9mJ. On the other hand, the input inductor energy is 8 mJ. The input inductor energy is reduced by 84% compared with the total inductor energy of the conventional two stage type. Therefore, the inductor volume of the boost inverter is reduced compared with the conventional two stage type. As a result, The volume of the DC/AC converter can be reduced using the boost inverter.

VI. EXPERIMENTAL RESULTS

Fig. 17 shows the experiment diagram of the boost inverter. The experimental condition is connected only resistor load in order to confirm the prototype system of the boost inverter. In

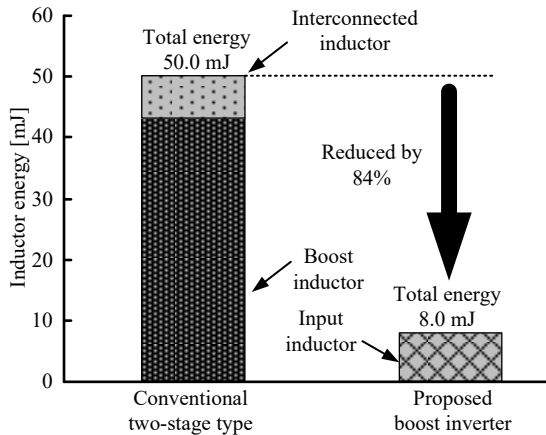


Fig. 16. Comparison of inductor energy between conventional two-stage type and boost inverter.

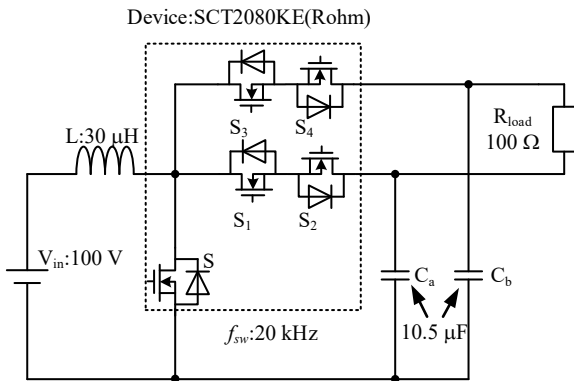


Fig. 17. Experimental circuit diagram using proposed circuit.

this case, the input inductor of the boost inverter is designed by (10). The input inductor value have 10% margin compared with the minimum design value in order to prevent the critical mode when the condition is the rated power.

Fig. 18 and 19 shows each operation waveform of the boost inverter when the output power is 100 W. It is confirmed the sinusoidal waveform of the output voltage at 100 V when the input power supply is DC source. In addition, the output current THD is measured 1.4%. The boost inverter is realized the low current THD of the output current. On the other hand, each output capacitor voltage is kept the constant value of the average voltage due to voltage control in order to become over the input voltage. Moreover, the output capacitor voltage is

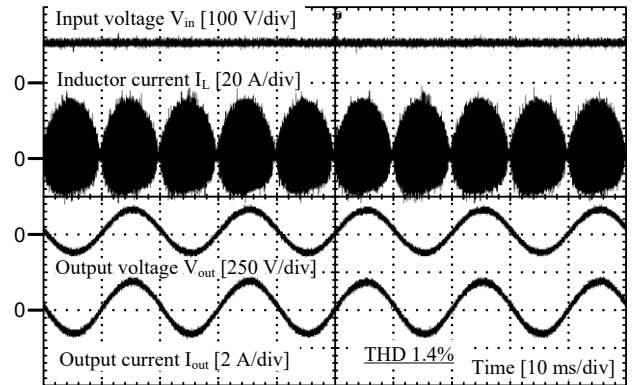


Fig. 18. Experimental results of input and output waveforms.

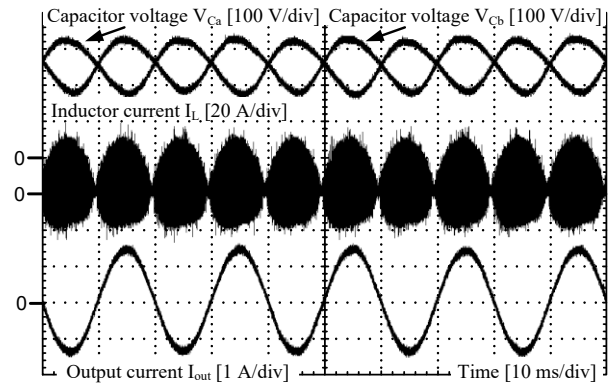


Fig. 19. Experimental waveform of each output capacitor voltage.

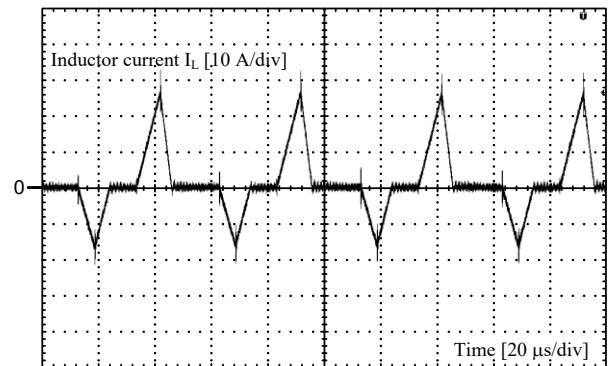


Fig. 20. Magnifying DCM waveform of input inductor current.

oscillated at the output frequency. As a results, it is confirmed the control of the boost inverter is operated.

Fig. 20 shows the magnified waveform of the inductor current. The input inductor current is operated in DCM due to zero current period. Therefore, there are zero current period d_0 between the voltage control of the output capacitor voltage V_{Ca} and V_{Cb} . It is confirmed the input inductor current similar to Fig. 6. In consequence, the input inductor current is shared between each output capacitor voltage control in the boost inverter. In addition, the inverter operation is realized by the boost inverter confirming from experimental results.

VII. CONCRUSION

In this paper, the boost inverter using only one input inductor is proposed applied for the micro-inverter in order to minimization of the volume. In addition, It is considered the design method of the input inductor, the simulation of the circuit operation and the comparing the losses of converter between the conventional two stage type and the proposed boost inverter. As a results, it is confirmed the inductor loss of the proposed boost inverter is reduced by 51.8% compared with the conventional topology in the theoretical consideration. Therefore, the operation of the boost inverter is confirmed in experimental results. In consequence, the proposed boost inverter can be converted DC to AC using only a input inductor. In the future, the operation and the efficiency of the boost inverter will confirm when the grid is connected at 300 W.

REFERENCES

- [1] S. Saridakis, E. Koutroulis, F. Blaabjerg : "Optimization of SiC-Based H5 and Conergy-NPC Transformerless PV Inverters", *IEEE Journal of Emerging and Selected Topics in Power Electronics*, Vol. 3, No. 2, pp. 555-567 (2015)
- [2] Y. Zhou, Hongbo Li, Hui Li : "A Single-Phase PV Quasi-Z-Source Inverter With Reduced Capacitance Using Modified Modulation and Double-Frequency Ripple Suppression Control", *IEEE Transactions on Power Electronics*, Vol. 31, No. 3, pp. 2166-2173 (2016)
- [3] R. Chattopadhyay, S. Bhattacharya, N. C. Foureaux, I. A. Pires, H. de Paula, L. Moraes, P. C. Cortizio, S. M. Silva, B. C. Fil-ho, Jose A. de S. Brito : "Low-Voltage PV Power Integration into Medium Voltage Grid Using High-Voltage SiC Devices", *IEEJ Journal of Industry Applications*, vol.4, no.6, pp.767-775, (2015).
- [4] S. Saridakis, E. Koutroulis, F. Blaabjerg : "Optimization of SiC-Based H5 and Con-ergy-NPC Transformerless PV Inverters", *IEEE Journal of Emerging and Selected Top-ics in Power Electronics*, vol. 3, no. 2, pp. 555-567, (2015).
- [5] S. Yamaguchi, T. Shimizu : "Single-phase Power Conditioner with a Buck-boost-type Power Decoupling Circuit", *IEEJ J. Industry Applications*, vol.5, no.3, pp.191-198, (2016).
- [6] C. Liao, W. Lin, Y. Chen, C. Chou : "A PV Micro-inverter With PV Current Decoupling Strategy", *IEEE Trans. on Power Electronics*, Vol. 32, No. 8, pp. 6544-6557 (2017).
- [7] M. A. Rezaei, K. Lee, A. Q. Huang : "A High-Efficiency Flyback Micro-inverter With a New Adaptive Snubber for Photovoltaic Applications", *IEEE Trans. on Power Electronics*, Vol. 31, No. 1, pp. 318-327 (2016)
- [8] A. C. Nanakos , G. C. Christidis , E. C. Tatakis : "Weighted Efficiency Optimization of Flyback Microinverter Under Improved Boundary Conduction Mode (i-BCM)", *IEEE Transactions on Power Electronics*, Vol. 30, No. 10, pp. 5548-5564 (2015)
- [9] W. J. Cha, Y. W. Cho , J. M. Kwon , B. H. Kwon : "Highly Efficient Microinverter With Soft-Switching Step-Up Converter and Single-Switch-Modulation Inverter", *IEEE Transactions on Industrial Electronics*, Vol. 62, No. 6, pp. 3516-3523 (2015)
- [10] D. Meneses , O. García , P. Alou, J. A. Oliver, J. A. Cobos : "Grid-Connected Forward Microinverter With Primary-Parallel Secondary-Series Transformer", *IEEE Transactions on Power Electronics*, Vol. 30, No. 9, pp. 4819-4830 (2015)
- [11] M. Jang, V. G. Agelidis : "A Minimum Power-Processing-Stage Fuel-Cell Energy System Based on a Boost-Inverter with a Bidirectional Backup Battery Storage", *IEEE Trans. on Power Electronics*, Vol. 26, No. 5, pp. 1568-1577 (2011).
- [12] R. O. Caceres, I. Barbi : "A boost DC-AC converter: analysis, design, and experimen-tation", *IEEE Transactions on Power Electronics*, vol. 14, no. 1, pp. 134-141, (1999).
- [13] D. B. W. Abeywardana, B. Hredzak, V. G. Agelidis : "An Input Current Feedback Method to Mitigate the DC-Side Low-Frequency Ripple Current in a Single-Phase Boost Inverter", *IEEE Transactions on Power Electronics*, vol. 31, no. 6, pp. 4594-4603, (2016).
- [14] W. Zhao, D. D. C. Lu, V. G. Agelidis : "Current Control of Grid-Connected Boost Inverter With Zero Steady-State Error", *IEEE Transactions on Power Electronics*, vol. 26, no. 10, pp. 2825-2834, . (2011).
- [15] Y. Tang, Y. Bai, J. Kan, F. Xu : "Improved Dual Boost Inverter With Half Cycle Modulation", *IEEE Transactions on Power Electronics*, vol. 32, no. 10, pp. 7543-7552, (2017).
- [16] T. Morita et al. : "650 V 3.1 mΩcm² GaN-based monolithic bidirectional switch using normally-off gate injection transistor", 2007 *IEEE International Electron Devices Meeting*, Washington, DC, 2007, pp. 865-868.
- [17] H. N. Le, K. Orikawa, J. I. Itoh : "Circuit-Parameter-Independent Nonlinearity Compensation for Boost Converter Operated in Discontinuous Current Mode", *IEEE Transactions on Industrial Electronics*, vol. 64, no. 2, pp. 1157-1166, (2017).